

Title No. 113-S32

Simplified Modeling of Frame Elements Subjected to Blast Loads

by Serhan Guner

A finite element method was recently proposed for the nonlinear analysis of plane frames subjected to impact, blast, and seismic loads. In this paper, numerical modeling studies are undertaken for 18 previously tested specimens to verify the accuracy, reliability, and practicality of this method for blast load conditions. Analysis results (obtained from this method and two other methods from the literature) are compared to the experimental responses in terms of peak displacements, stiffnesses, residual displacements, and crack widths. The three main advantages of the proposed method are demonstrated: more accurate modeling of reinforced concrete behavior by using pre-implemented default material models, simpler modeling requirements, and shorter analysis times. The proposed method was found to simulate the experimental behavior of the specimens examined with a high degree of accuracy. The explicit three-parameter time integration algorithms implemented provide unconditional numerical stability and require significantly shorter analysis times than continuum finite element methods.

Keywords: blast; fibers; finite elements; frame; modeling; nonlinear analysis; shear; strain rates; time-history analysis.

INTRODUCTION

Owing to recent terror incidents, structural resilience to blast explosions has become a crucial design requirement for government and high-profile public buildings. Analysis software available in the literature for blast loads ranges from simplified “single-degree-of-freedom” (SDOF) tools to complex “continuum finite element analysis” (FEA) software. The SDOF tools, such as SBEDS (PDC 2015), are easy to use and directly provide the required design parameters, such as the maximum displacements and reactions; consequently, they are commonly used in practice for structural design. These tools, however, are only suited for the analysis of single structural elements with simple boundary conditions and neglect many important influences, such as the interaction of shear, axial, and bending effects; changing axial loads; membrane action; and hysteretic material response. On the other hand, FEA software, such as LS-DYNA (2015) and ABAQUS (2015), is more comprehensive but demands extensive knowledge and experience, requires a large number of input parameters, and takes significant time. Because these tools are designed as general-purpose analysis tools for many materials, they require significant customization for modeling reinforced concrete. The accuracy of the results obtained from these tools is highly dependent on how the concrete modeling parameters are input. Consequently, continuum FEA software is primarily used for academic studies. Thus, there remains a significant need for the development of practical but accurate analysis tools that can be used by structural engineers in practice for the analysis of frame structures under blast pressures.

In response to this need, an analysis method was developed by Guner and Vecchio (2012) and implemented into an existing frame analysis program—VecTor5 (Guner and Vecchio 2008)—for impact, blast, and seismic loads. In addition to accurately modeling the concrete response and shear behavior, it sought to eliminate the need for pre-analysis material model calculations and the selection of analysis options. This was achieved by developing a specialized method solely for concrete frames, in which the most suitable analysis options and concrete parameters were pre-implemented as the default options. In addition to simplifying the modeling process, the default options establish a single solution for a given problem.

OBJECTIVE AND SCOPE

The objective of this study is to demonstrate the application and verification of a recently developed method (Guner and Vecchio 2012) for blast load analysis, and numerically study the dynamic behavior of previously tested frame elements. The literature is very limited in experimental blast studies due to the high cost and security issues involved. After a comprehensive literature review, four studies, including 18 specimens, were identified suitable for modeling with the proposed analysis method. The specimens include 10 singly reinforced and four doubly reinforced panels, two wall strips, one square slab, and one prestressed panel. Some of the specimens were tested multiple times, thereby providing a total number of 24 simulations. The materials modeled include both high-strength and normal-strength concrete in combination with high-strength vanadium reinforcing bars, normal-strength deformed reinforcing bars, and low-relaxation prestressing tendons. Throughout the analyses, only the default material models and analysis options were used.

This paper provides a brief overview of the analysis method, summarizes the experimental programs, and presents the numerical modeling details. The numerical responses obtained are compared to the experimental behaviors. Critical modeling aspects, such as the time step length, strain rate effects, and shear effects, are also examined.

RESEARCH SIGNIFICANCE

Recent bomb attacks on high-profile buildings have created an increased awareness and demand for blast-resistant structures. The methods commonly employed for blast load

ACI Structural Journal, V. 113, No. 2, March-April 2016.

MS No. S-2015-030.R1, doi: 10.14359/51688064, received May 3, 2015, and reviewed under Institute publication policies. Copyright © 2016, American Concrete Institute. All rights reserved, including the making of copies unless permission is obtained from the copyright proprietors. Pertinent discussion including author's closure, if any, will be published ten months from this journal's date if the discussion is received within four months of the paper's print publication.

analysis are either based on overly-simplistic “single-degree-of-freedom” (SDOF) approaches or overly-complex “finite element analysis” (FEA) software. SDOF approaches have limited applicability and fail to accurately model the behavior of reinforced concrete. FEA software is time-consuming, demands significant knowledge, and requires a large number of customized input parameters for reliable results. This study examines the accuracy, reliability, and practicality of a recently proposed analysis method by modeling 18 previously tested specimens using only the default material models and analysis options.

OVERVIEW OF PROPOSED ANALYSIS METHOD

The proposed method employs six-degree-of-freedom line elements, as shown in Fig. 1(a), within a distributed-plasticity frame analysis framework using an iterative, total-load, secant-stiffness formulation. The nonlinear sectional analysis algorithms developed provide a comprehensive and accurate representation of the concrete response, including the shear effects coupled with axial and flexural responses, based on the Disturbed Stress Field Model (Vecchio 2000). A fiber discretization of the cross section is employed as illustrated in Fig. 1(b). Each concrete and longitudinal reinforcing bar layers is defined as discrete elements; the transverse and out-of-plane reinforcement is smeared within the concrete layers. The out-of-plane reinforcement provides confinement to concrete layers. The main sectional compatibility requirement is that “plane sections remain plane,” while the sectional equilibrium requirements include balancing the axial force, shear force, and bending moment (calculated by the global frame analysis). A parabolic shear strain distribution through the section depth is assumed. To compensate for the clamping stresses in the transverse direction (assumed to be zero), a shear protection algorithm is developed to prevent premature failures of D-regions.

The effects of high strain rates are considered through a dynamic increase factor approach. For concrete, the compressive and tensile strengths, the modulus of elasticity, and the peak strain corresponding to the peak stress are enhanced using the *fib* Model Code (2010) formulations. For reinforcing steel, the yield and ultimate stresses are increased using the Malvar (1998) formulations. The method requires the input of the static material properties, to which the dynamic increase factors are applied continuously during an analysis using the calculated strain rates at each time step. Further details on strain rate formulations are provided in Guner and Vecchio (2012).

An explicit three-parameter time integration method was developed and implemented into the proposed method, which allows the use of either Newmark’s Average Acceleration, Newmark’s Linear Acceleration (Newmark 1959), or Wilson’s Theta (Wilson et al. 1972) methods. Structural damping is primarily taken into account through the nonlinear concrete and reinforcement hysteresis models incorporated, as presented in Guner and Vecchio (2011). Supplemental viscous damping can be defined using either the Rayleigh or alternative damping formulations implemented. The method allows for the analysis of frames with unusual or complex cross sections, and inherently considers significant second-order mechanisms such as the membrane action, concrete

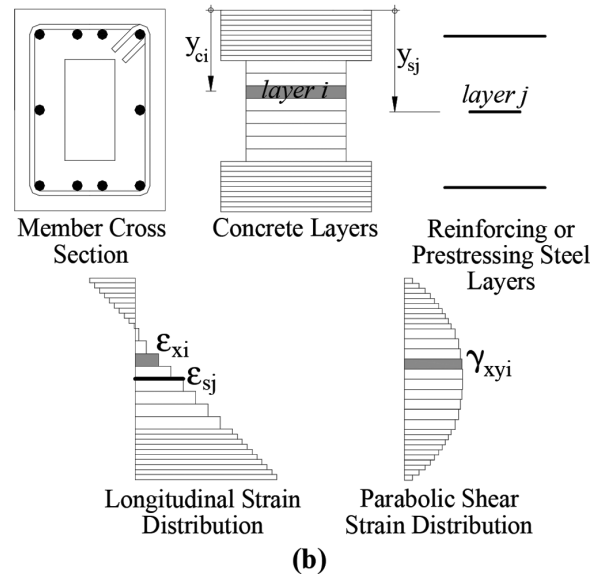
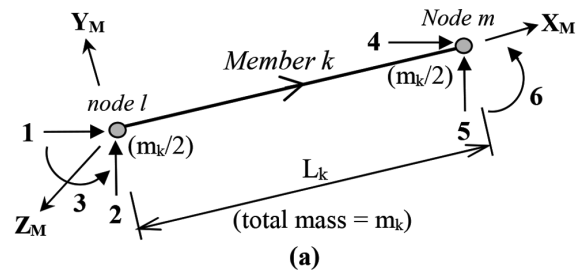


Fig. 1—(a) Frame element proposed; and (b) layered section method proposed.

out-of-plane confinement effects, reinforcement buckling, and reinforcement dowel action. The formulation details are provided in Guner and Vecchio (2010a,b; 2011; 2012).

MODELING PARAMETERS

The numerical models were created through graphical preprocessor software FormWorks-Plus (Sadeghian 2012) using the basic structural information, including the geometry, support conditions, cross section details, concrete strengths, and reinforcement grades. The default models were used for the material modeling throughout this study (refer to Table 1). Figure 2(a) presents the default concrete hysteresis model. More details on these models can be found in Wong et al. (2013). Geometric nonlinearity and the previous loading history were also considered by default.

The only material model selection performed was for the concrete pre-peak compression response, which is dependent on the concrete strength used. The Popovics normal-strength concrete (NSC) and high-strength concrete (HSC) formulations were used throughout this study. The only required input parameter was the uniaxial concrete strength f'_c . The other concrete parameters were calculated using Eq. (1) and (2), where E_c is the modulus of elasticity, ϵ_0 is the strain corresponding to f'_c , and f'_t is the cracking stress, in MPa.

$$E_c = 3300\sqrt{f'_c} + 6900 \text{ (in MPa)}$$

$$\text{and } \epsilon_0 = \frac{f'_c}{E_c} \left(\frac{n}{n-1} \right), \text{ where } n = 0.80 + \frac{f'_c}{17} \quad (1)$$

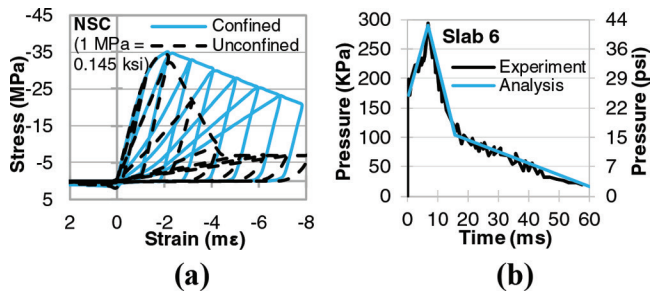


Fig. 2—(a) Concrete hysteresis model; and (b) typical blast pressure input.

$$f'_t = 0.33\sqrt{f'_c} \quad (\text{in MPa}) \quad (2)$$

Wilson's Theta method, which is the default time integration method, was used in all analyses with no additional viscous damping defined (with the exception of the Texas panels, as discussed later). The time-step length was selected to be approximately equal to the smallest natural vibration periods of the specimens. The out-of-plane reinforcement, which is the secondary reinforcement in the z-direction, was assigned into the concrete layers within a tributary distance of approximately six to seven times the bar diameter.

The developed method requires the input of the blast pressure history with a trilinear idealization; one sample input is presented in Fig. 2(b). These histories were obtained from experimental studies in the literature. In these studies, the blast loading was generated using shock tubes, which create shock waves with a uniform pressure applied on each specimen. In the case of an internal explosion involving blast wave reflections (not considered in this study), the proposed method can still be used, provided that the resulting pressure history is calculated and supplied as input.

The analysis results were obtained through the graphical post-processor software Janus (Chak 2013). The results investigated included the load-deflection responses, member deformations, concrete crack widths, reinforcement stresses and strains, the failure modes, and the failure displacements. The post-peak responses were also obtained and presented, from which the energy dissipation and the displacement ductilities were calculated.

SINGLY REINFORCED PANEL SPECIMENS

The first set of specimens examined was that tested by Thiagarajan and Johnson (2014), involving 12, one-third-scale, one-way panels tested in a compressed gas-driven blast load simulator at the Engineer Research and Development Center (ERDC) located in Vicksburg, MS. The slabs had the dimensions of 1625 x 857 x 102 mm (64 x 33.75 x 4 in.) and were supported in the longitudinal direction by steel sections with a depth of 152.4 mm (6 in.) at the top and bottom, which left a clear span of 1320 mm (52 in.). The main variable was the concrete strength, with either 34.5 or 80 MPa (5 or 11.6 ksi), and the longitudinal reinforcement spacing of either No. 3 bars at 101.6 mm (4 in.) or No. 3 bars at 203.2 mm (8 in.). All panels had five No. 3 bars, with 9.5 mm (0.375 in.) diameter, at a spacing of 304.8 mm (12 in.) in the transverse direction as the shrinkage reinforcement. The concrete cover used was 12.7 mm (0.5 in.). The odd-

Table 1—Default material models

Material behavior	Default model
Compression base curve	Popovics (NSC) or (HSC)
Compression post-peak	Modified Park-Kent
Compression softening	Vecchio 1992-A
Tension stiffening	Modified Bentz 2003
Tension softening	Linear
Confinement strength	Kupfer/Richart
Concrete dilatation	Variable – orthotropic
Cracking criterion	Mohr-Coulomb (Stress)
Crack width check	Agg/5 max crack width
Concrete hysteresis	Nonlinear with plastic offsets
Slip distortion	Walraven
Strain rate effects	fib Model Code – Malvar
Reinforcing bar hysteresis	Seckin with Bauschinger
Reinforcing bar dowel action	Tassios (crack slip)
Reinforcing bar buckling	Refined Dhakal-Maekawa

numbered slabs had HSC with 101.6 mm (4 in.) bar spacing for Slabs 1, 3 and 5, and 203.2 mm (8 in) bar spacing for Slabs 7, 9 and 11. The even-numbered slabs had NSC with 101.6 and 203.2 mm (4 and 8 in.) bar spacing for Slabs 2, 4 and 6, and for Slabs 8, 10 and 12, respectively. The high-strength panels used 572 MPa (83 ksi) high-strength, low-alloy vanadium reinforcement (VR), and the normal-strength panels used 469 MPa (68 ksi), Grade 60 conventional reinforcement (NR). The slabs were subjected to very-high-peak reflected blast pressures and impulses ranging from 0.36 MPa (52.2 psi) and 6.99 MPa-ms (1014 psi-ms) to 0.23 MPa (33.4 psi) and 3.41 MPa-ms (495 psi-ms). More details on this experimental program can be found in Shetye (2013).

The frame model for the slabs was created for one-half of the specimens benefiting from the symmetry, as presented in Fig. 3. The model includes 14 elements, each with a length of approximately one-half of the cross section depth. The x- and y-degrees of freedom at Node 3 were restrained to define a pin; the x- and z-degrees of freedom of Node 15 were restrained to satisfy the condition of symmetry.

The sectional models were created using 34 concrete layers, with a constant layer thickness of 3 mm (0.12 in.), and one discrete steel layer. The shrinkage reinforcement was smeared into the concrete layers as the out-of-plane reinforcement ρ_z within a tributary width of 75 mm (3 in.), as shown in Fig. 3. The transverse reinforcement ratio was defined as zero. The concrete compressive strength and steel properties were used as reported in Shetye (2013) and Thiagarajan et al. (2011), respectively. The maximum aggregate size used in the analyses was taken as zero for the high-strength specimens as cracks pass through, rather than going around the aggregate, causing aggregate interlock to be ineffective.

The time-step length was determined as a result of a parametric study. As presented in Fig. 4, the computation time exponentially increases for the time-step lengths smaller than a certain value, while the analysis results are not affected as much. Consequently, the optimum time-step length was

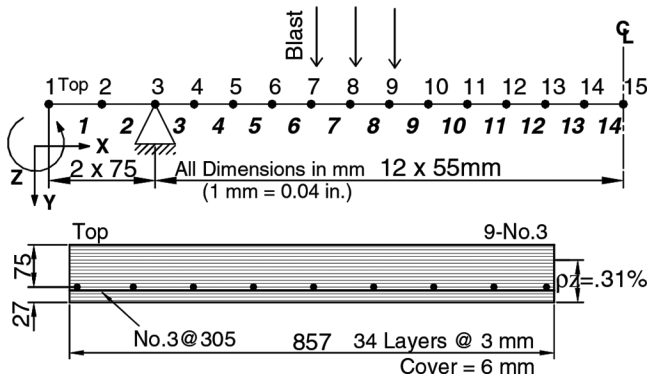


Fig. 3—Singly reinforced panels: frame and sectional models.

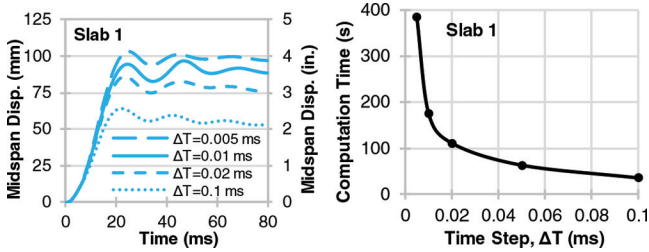


Fig. 4—Singly reinforced panels: effects of time-step length.

determined to be 0.01 ms, and was used in the analyses. The smallest natural vibration period of the specimens was calculated to be approximately 0.03 ms at the 27th mode for information purposes. A trilinear pressure input was used, with a sample presented in Fig. 2(b).

Discussion of responses

As presented in Fig. 5, the calculated midspan displacement responses captured the experimental behaviors well in terms of peak displacements, stiffnesses, and residual displacements. Slabs 2, 4, and 6 experienced concrete crushing over nine layers in the analyses, which is consistent with the experimental observations reported by Thiagarajan and Johnson (2014). A photograph of Slab 4 taken at the end of the test is shown in Fig. 6. The calculated peak reinforcement strains ranged from 40 to 55 me, and the calculated maximum residual crack widths ranged from 6 to 8 mm (0.24 to 0.32 in.). Slabs 3 and 7 are excluded from this study due to apparent irregularities in the recorded displacement data.

Considering all 10 slabs, a mean of 1.02 and a coefficient of variation (COV) of 12% were obtained for the calculated-to-observed peak displacement ratios, as listed in Table 2. The same slabs were modeled using the LS-DYNA software by Shetye (2013). These models included constant-stress, eight-noded hexahedron elements, with two different meshes—namely, 25.4 and 12.7 mm (1 and 0.5 in.)—in combination with two different concrete models—namely, Concrete Damage Model Release 3 (CDMR3) and Winfrith Concrete Model (WCM). Using the peak displacement values reported, the mean and COV values were found to be 1.10 and 11% for the CDMR3, and 0.90 and 15% for the WCM for the same 10 slabs (refer to Table 1).

To assess the influence of the strain rate and shear effects, parametric studies were conducted for one HSC and one NSC panel. As presented in Fig. 7, the consideration of

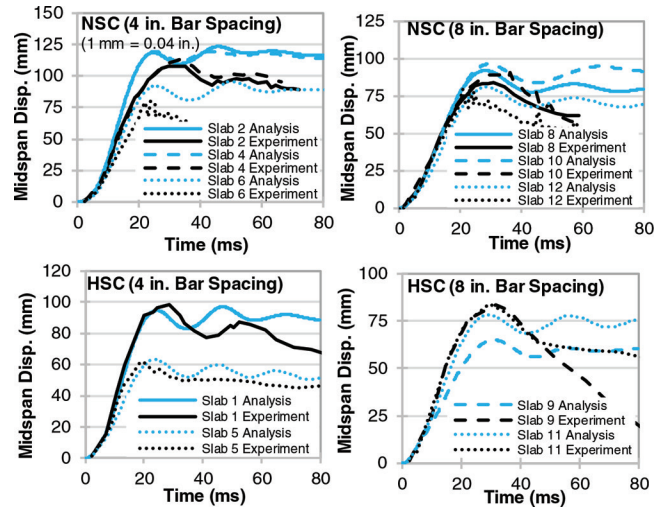


Fig. 5—Singly reinforced panels: midspan deflection responses.

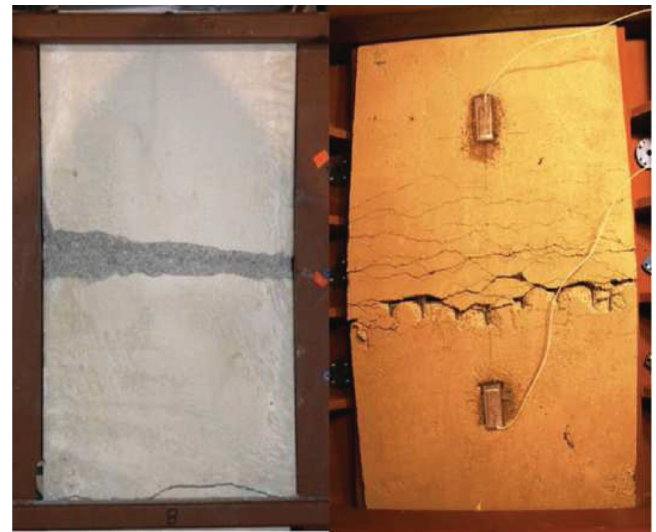


Fig. 6—Singly reinforced panels: back and front side views of Slab 4 (Thiagarajan and Johnson 2014).

strain rate effects reduced the peak slab displacement by 7% for the HSC, and 16% for the NSC. The effect of shear on the global responses were found to be insignificant, with 2% and 5% change in the peak displacements for the HSC and NSC slabs, respectively, which was expected due to the slender nature of the slab specimens.

DOUBLY REINFORCED PANEL SPECIMENS

The second series of slabs examined was that tested by Robert and Johnson (2009), involving 10, one-third-scale, one-way panels tested at the ERDC in Vicksburg, MS. The slab dimensions and support conditions were the same as the singly reinforced panels discussed previously. These slabs incorporated double mat reinforcement with either conventional 469 MPa (68 ksi), Grade 60 (NR) or 572 MPa (83 ksi) vanadium reinforcing bars (VR) in combination with 27.6 MPa (4 ksi) (NCS) or 107 MPa (15.5 ksi) (HSC) concrete. Examined herein are the four panels for which the experimental blast pressure and midspan displacement histories were available. Slabs 3 and 5 consisted of HSC, with

Table 2—Comparison of analysis and experiment results

	Test	Analysis	Ratio	CMDR3	Ratio	WCM	Ratio
Slab 2	109.0	123.4	1.13	120.1	1.10	83.8	0.77
Slab 4	113.0	119.4	1.06	113.0	1.00	83.1	0.73
Slab 6	80.5	95.5	1.19	88.1	1.09	54.1	0.67
Slab 8	85.3	91.9	1.08	92.7	1.09	71.1	0.83
Slab 10	91.4	96.2	1.05	101.1	1.11	83.6	0.91
Slab 12	80.5	80.6	1.00	86.9	1.08	76.5	0.95
Slab 1	98.8	97.1	0.98	96.5	0.98	97.3	0.98
Slab 5	62.5	63.0	1.01	85.9	1.37	74.7	1.20
Slab 9	86.4	64.9	0.75	88.6	1.03	82.6	0.96
Slab 11	85.9	78.3	0.91	98.6	1.15	82.6	0.96
		Mean	1.02		1.10		0.90
		COV	0.12		0.11		0.15
Slab 3	122.0	117.8	0.97	101.0	0.83	76.0	0.62
Slab 5	140.0	128.7	0.92	121.0	0.86	124.0	0.89
Slab 6	129.0	132.0	1.02	129.0	1.00	137.0	1.06
Slab 9	212.0	135.8	0.64	142.0	0.67	160.0	0.75
		Mean	0.89		0.84		0.83
		COV	0.17		0.12		0.16
	Test	Analysis	Ratio	SDF	Ratio		
CS1-1	26.1	29.5	1.13	30.3	1.16		
CS1-2	167.8	166.1	0.99	137.3	0.82		
CS2-1	16.3	16.4	1.00	16.0	0.98		
CS2-2	148.9	140.4	0.94	105.7	0.71		
CS3-1	6.9	6.0	0.88	8.9	1.29		
CS3-2	16.3	15.8	0.97	18.6	1.14		
CS3-3	197.5	199.6	1.01	217.8	1.10		
		Mean	0.99		1.03		
		COV	0.08		0.20		
TX-1	6.7	9.5	1.42	12.4	1.85		
TX-2	24.0	31.0	1.29	29.0	1.21		
TX-3	65.8	71.8	1.09	94.5	1.44		
		Mean	1.27		1.50		
		COV	0.16		0.33		

high-strength and normal-strength reinforcement, respectively. Slabs 6 and 9 had NSC, and high-strength and normal-strength reinforcement, respectively. The slabs were subjected to very-high-peak reflected blast pressures and impulses ranging from 0.35 MPa (50.8 psi) and 6.79 MPa-ms (985 psi-ms) to 0.39 MPa (56.6 psi) and 7.71 MPa-ms (1118 psi-ms).

The frame and sectional models created were the same as the singly reinforced panels with the exception of double layers of main and shrinkage reinforcement, as shown in Fig. 8.

Discussion of responses

As presented in Fig. 9, the midspan displacement responses were calculated reasonably accurately with a mean of 0.89 and a COV of 17%. The somewhat-high scatter in the calcu-

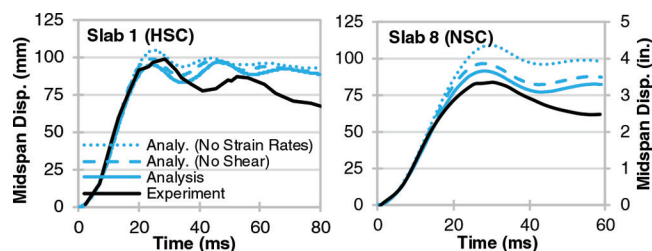


Fig. 7—Singly reinforced panels: effects of strain rates and shear.

lations was caused by Slab 9. The use of high-strength reinforcement significantly reduced the peak displacement, by approximately 40%, in the experiment (note the experimental responses of Slabs 6 and 9, both of which were

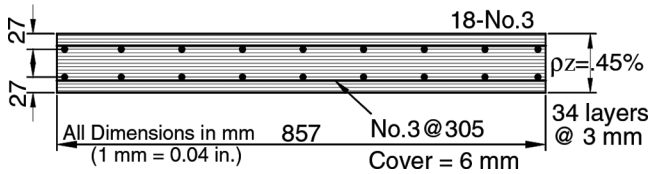


Fig. 8—Doubly reinforced panels: sectional model.

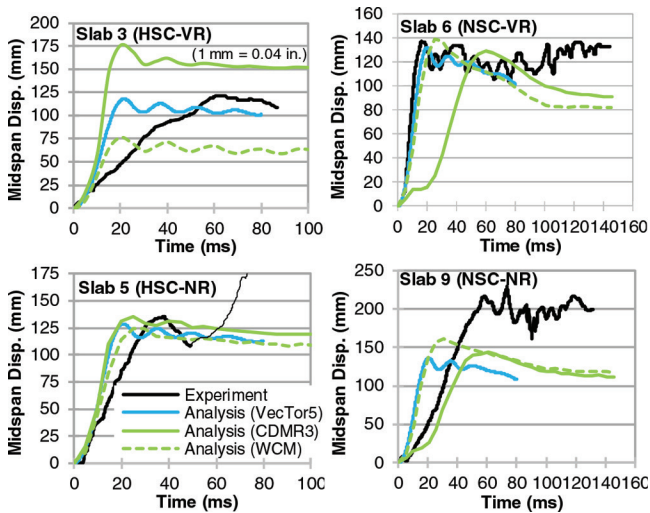


Fig. 9—Doubly reinforced panels: midspan deflection responses.

subjected to similar blast loads). In the analyses, both slabs exhibited similar responses due to the very similar stress-strain responses of both types of reinforcing bars (refer to Fig. 10). When this analysis is excluded, the mean and COV values became 0.97 and 5.2%, respectively. The ascending branch of the experimental displacement response of Slab 5 after the peak displacement was excluded, as shown with a thinner line. The calculated peak reinforcement strains were in the range of 30 mε, and the calculated maximum crack width was approximately 4.5 mm (0.18 in.). Only the maximum crack widths were reported in the experimental study as 4.2 mm (0.17 in.), which agrees well with the numerical responses. The analysis time was less than 200 seconds on a notebook computer with a dual-core 1.8 GHz processor.

The same panels were modeled by Thiagarajan et al. (2015) with the FEA software LS-DYNA (2015), using two meshes and two concrete models as previously discussed. The analyses required significant material model input and analysis option selections conducted as a part of a master's study by Vasudevan (2012). Shown in Fig. 9 are the numerical responses reported for the 25.4 mm (1 in.) mesh, which appears to be somewhat more accurate than the 12.7 mm (0.5 in.) mesh (not shown herein). The peak displacement of Slab 9 is also significantly underestimated in this study. The analysis time reported was 600 seconds for the 25.4 mm (1 in.) mesh, and 1500 s for the 12.7 mm (0.5 in.) mesh on a computer with unknown specifications.

OTTAWA SPECIMENS

Another series of specimens examined was that tested by Jacques (2011), involving 13, large-scale, one-way wall strips and two-way slabs. Considered herein are the one-way and unretrofitted specimens. Specimens CS1 and CS2

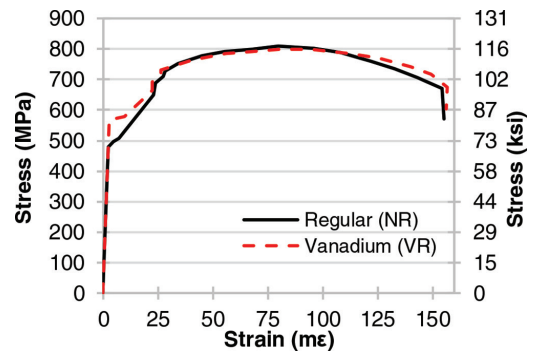


Fig. 10—Doubly reinforced panels: experimental response of reinforcement.

consisted of simply supported, one-way wall strip panels with a length of 2440 mm (96.1 in.), a clear span of 2232 mm (87.9 in.), and a width of 440 mm (17.3 in.). The panel thicknesses were 80 and 120 mm (3.15 and 4.7 in.) for CS1 and CS2, respectively. The panels were doubly reinforced with four 6.3 mm (0.25 in.) diameter steel reinforcing bars having a yield strength of 580 MPa (84 ksi) in the longitudinal direction, and had a clear cover of 6 mm (0.24 in.). The concrete mixture was reported to have 10 mm (0.4 in.) crushed limestone aggregate, and a compressive strength of 59.5 MPa (8.6 ksi) on the day of testing. Each panel was tested twice, subjected to two blast loads. The peak reflected blast pressures and impulses were reported to be 12.4 kPa (1.8 psi) and 95.9 kPa-ms (13.9 psi-ms), and 42.7 kPa (6.2 psi) and 301.3 kPa-ms (43.7 psi-ms) for the first and second tests of CS1 (CS1-1 and CS1-2); 17.9 kPa (2.6 psi) and 142.7 kPa-ms (20.7 psi-ms) for CS2-1; and 57.9 kPa (8.4 psi) and 382.7 kPa-ms (55.5 psi-ms) and for CS2-2. Due to the width of the shock tube opening being larger than the width of the specimens, a load transfer device consisting of a light-gauge, steel-sheet metal skin (covering the entire height and width of the shock tube test frame) was used. The device added a weight of 394 kg (869 lb) to the specimens. This device was reported to only transfer the positive blast pressures onto the specimens due to the separation from the specimens during the negative loading phases.

CS3 consisted of a simply supported, one-way slab with a length of 2440 mm (96.1 in.), a clear span of 2232 mm (87.9 in.), a width of 2440 mm (96.1 in.), and a thickness of 75 mm (3 in.). It was doubly reinforced in both directions, with eleven 6.3 mm (0.25 in.) diameter steel reinforcing bars having a yield strength of 580 MPa (84 ksi), and had a concrete cover of 6 mm (0.24 in.). The concrete strength on the day of testing was reported to be 60 MPa (8.7 ksi). The specimen was tested three times. The peak reflected blast pressures and impulses reported were 15.2 kPa (2.2 psi) and 123.4 kPa-ms (17.9 psi-ms) for CS3-1; 28.3 kPa (4.1 psi) and 204.1 kPa-ms (29.6 psi-ms) for CS3-2; and 100.7 kPa (14.6 psi) and 770.2 kPa-ms (111.7 psi-ms) for CS3-3. More details on this experimental program can be found in Jacques (2011).

The frame model was created using 20 elements and a pin support at Node 3. The sectional models included 32 layers for CS1 and CS2, and 30 layers for CS3, as shown in Fig. 11. The reinforcement in the unsupported slab direction of CS3

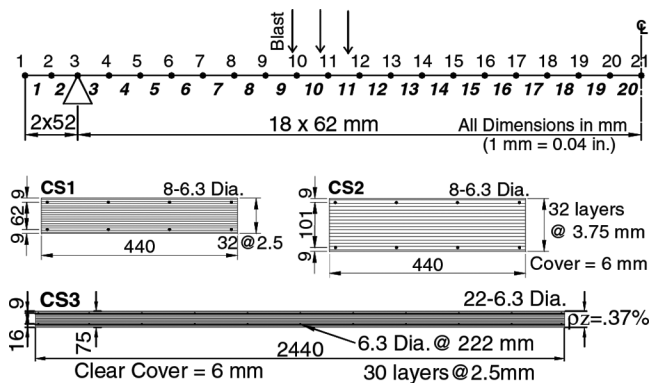


Fig. 11—Ottawa panels: frame and sectional models.

was modelled as the out-of-plane reinforcement with a ratio of $31.2 \times 2 / (222 \times 75) = 0.37\%$. The steel properties were obtained from the standard coupon test results reported in Jacques (2011).

A time-step length of 0.05 ms was used in all analyses, which was approximately equal to the smallest natural vibration period of the specimens (approximately 0.04 ms at the 40th mode for all three specimens). A trilinear pressure input was used in the analyses, with all negative blast pressures taken zero for CS1 and CS2, as recommended in Jacques (2011).

Discussion of responses

As shown in Fig. 12, the midspan deflection responses of all specimens were captured very well in terms of the peak displacements and stiffnesses. For all seven analyses, a mean of 0.99 and a COV of 8% were obtained for the calculated-to-observed peak displacement ratios. The only discrepancy obtained was for the post-peak displacement responses of CS3-1 and CS3-2. The blasts pressures applied to these specimens included significant post-peak branches, as shown in Fig. 13. The trilinear blast pressure input was insufficient to model this type of loading, causing these discrepancies in the post peak-responses. This is typically not a concern in practice, where most blast loads are considered only with one positive and one negative phase that can be modeled with a trilinear blast pressure input. The calculated maximum midspan crack widths were in the range of 0.3 mm (0.01 in.) for CS1-1 and CS2-1 (reported as minor cracking in the experimental study), and 4 and 6 mm (0.16 and 0.24 in.) for CS1-2 and CS2-2 (reported as major cracking in the experimental study), respectively. The maximum crack widths calculated for CS3 were 0.1, 0.3, and 4 mm (0.004, 0.01, and 0.16 in.) for Tests 1, 2, and 3, respectively. For the second and third analyses of previously damaged beams, a mean of 0.98 and a COV of 3% were obtained for the calculated-to-observed peak displacement ratios. Given the scarcity of analysis tools capable of considering the previous loading and damage, this capability of the developed analysis method is noteworthy. The analysis time required was in the range of 200 s on notebook computer with a dual-core 1.8 GHz processor.

The same specimens were modeled in Jacques (2011) using the explicit solution of the SDOF dynamic equation of motion including the concrete confinement and strain rate effects. These analyses calculated the midspan displacement histories

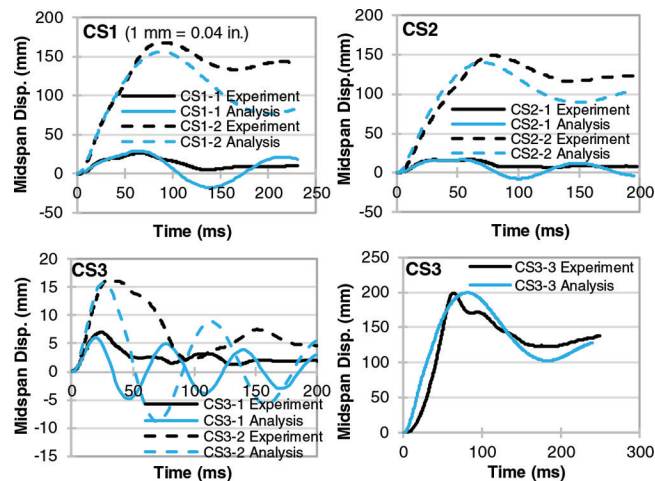


Fig. 12—Ottawa panels: midspan deflection responses.

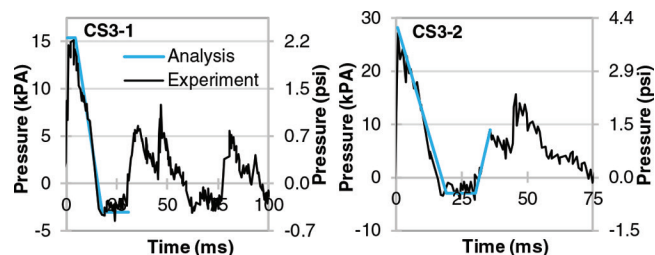


Fig. 13—Ottawa panels: blast pressure histories.

up to the peak displacement, as listed in Table 1. For these three panels, the SDOF analyses yielded a mean of 1.03 and a COV of 20% for the calculated-to-observed peak displacement ratios.

TEXAS SPECIMENS

The last series of specimens examined was that tested by Dunkman et al. (2009), involving one pre-tensioned and one post-tensioned, large-scale, one-way panels tested at the ABS testing facility in Bulverde, TX. The panels had a length of 2578 mm (101.5 in.), a clear span of 2438 mm (96 in.), a width of 1029 mm (40.5 in.), and a thickness of 89 mm (3.5 in.). The panels were wedged between stiffened steel angles and shimmed with wood blocks with the intention of creating simple supports. The panels had a concrete strength of 30.8 MPa (4.5 ksi) and a maximum nominal aggregate size of 9.5 mm (0.375 in.). The prestressed panel had three 12.7 mm (0.5 in.) diameter, Grade 270, low-relaxation strands stressed to 138 kN (31 kip), and four No. 4, Grade 60 reinforcing bars at its middepth. Four No. 4, Grade 60 reinforcing bars were also provided for shrinkage control in the short direction with a spacing of 304.8 mm (12 in.). Both panels were tested side-by-side, subjected to three blast pressures with the peak reflected pressures and impulses of 43.4 kPa (6.3 psi) and 289.6 kPa-ms (42 psi-ms), 71.7 kPa (10.4 psi) and 551.6 kPa-ms (80 psi-ms), and 75.8 kPa (11 psi) and 1310.0 kPa-ms (190 psi-ms), respectively.

The prestressed panel was modeled in this study because the proposed method is currently suitable for modeling reinforced and prestressed concrete elements. The frame model created included 25 elements and a pin support idealization, as shown in Fig. 14. The sectional models were created using 30 concrete layers, in which the out-of-plane reinforcement was

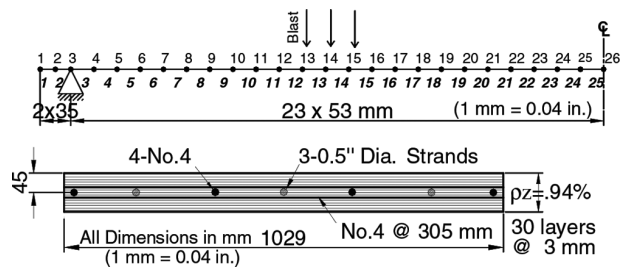


Fig. 14—Texas panels: frame and sectional models.

smear with a ratio of $2 \times 129 / (305 \times 90) = 0.94\%$. The low-relaxation tendon properties were input as an area of 98.7 mm^2 (0.15 in.^2), an ultimate strength of 1860 MPa (270 ksi), a yield stress of 1690 MPa (245 ksi), and a locked-in strain difference of $7.0 \text{ m}\epsilon$. As indicated in Dunkman et al. (2009), 7% prestressing loss and a corresponding effective modulus of elasticity of $182,800 \text{ MPa}$ ($26,513 \text{ ksi}$) were used. For the No. 4 reinforcing bars, an area of 129 mm^2 (0.20 in.^2) and a yield stress of 450 MPa (65.3 ksi) were used as reported. The ultimate stress and strain values were assumed to be 620 MPa (90 ksi) and $8 \text{ m}\epsilon$, respectively.

Due to the low blast pressures applied, essentially linear-elastic behaviors were expected under the first and second loads. For the numerical simulations where insignificant nonlinearity take place, the energy dissipated by the material hysteresis models becomes insufficient, thereby requiring the use of some supplemental viscous damping. Consequently, supplemental viscous damping ratios of 1% and 2% were assigned to the vibration Modes 1 and 3. The assigned ratios were kept small to avoid dissipating excessive energy and obtaining unconservative results. A time-step length of 0.02 ms was used, which was equal to the smallest natural vibration period of the specimens. The reflected pressure histories reported in Dunkman et al. (2009) were used in the analyses with a trilinear idealization.

Discussion of responses

As shown in Fig. 15, the peak midspan displacements were captured reasonably well. The overestimation for the first two analyses was expected due to the pin supports used in the analyses; the supports behaved as partially restrained in the experiments, as reported by Dunkman et al. (2009). The analyses indicated no cracking, and minor cracking with 0.5 mm (0.02 in.) maximum crack widths under the first and second blast loads, which is consistent with the experimental observations. The third blast load caused extensive and visible cracking in the experiment, which was captured by the analysis with a 1.2 mm (0.05 in.) maximum crack widths. The discrepancies in the post-peak displacement calculations stemmed from the trilinear loading idealization,

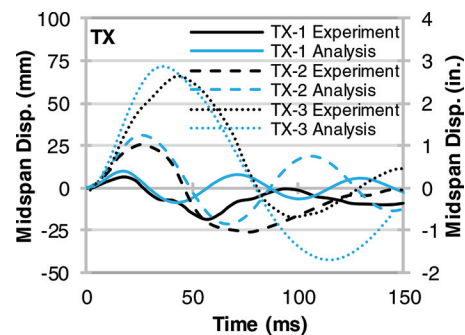


Fig. 15—Texas panels: midspan deflection responses.

which was not sufficient to model the negative and second positive phases of the experimental blast pressure histories.

These specimens were modeled in Dunkman et al. (2009) using a simply supported SDOF model. Their study only provided the peak midspan displacement values without displacement histories, as listed in Table 1. For these three analyses, they calculated the peak midspan displacements with a mean of 1.50 and a COV of 33% . Note the significant overestimation and variation in the calculations by the SDOF model.

SUMMARY AND CONCLUSIONS

A recently developed nonlinear finite element analysis method was verified by conducting numerical modeling studies for 18 previously tested specimens subjected to shock-tube-induced blast pressures. Four specimens were subjected to multiple blasts, resulting in 24 simulations in total. Most specimens were subjected to very-high-peak reflected pressures in the range of 0.35 MPa (50 psi) and exhibited significant damage and nonlinearity. The reflected blast pressures and displacement histories were obtained from the publications cited, and compared to the computed responses.

An explicit three-parameter time integration method was used by the developed method through a total-load, secant-stiffness formulation. Rigorous nonlinear sectional analyses were undertaken, considering the strain rate effects using a dynamic increase factor approach, and using the realistic concrete and reinforcement hysteresis models implemented. Shear effects were included through a two-dimensional implementation of the Disturbed Stress Field Model, which is based on a smeared, rotating crack conceptualization. Through this study, the three main advantages of the proposed method were demonstrated: the accurate modeling of reinforced concrete behavior using the default options; the simple modeling requirements that make it suitable for practical applications; and short analysis times. The results of this study support the following conclusions:

1. Nonlinear blast load analysis of frame elements requires comprehensive and fast analysis tools. Graphical pre- and post-processor software is essential in verifying the

structural models and making sense of the megabytes of the output data produced.

2. The general-purpose finite element analysis software available in the literature demands expert knowledge, requires a large number of input parameters and pre-analysis calculations, and takes significant time. The accuracy obtained is highly dependent on the material model parameter input. For the 10 analyses considered in this study, WCM provided a reasonable mean of 0.88 and COV of 16% for the calculated-to-observed midspan displacement ratios. The volume of the two master's theses, which include the details of these analyses, demonstrate the pre-analysis calculations and the effort required. Each analysis was reported to take 600 seconds for the model with a 25.4 mm (1 in.) mesh, and 1500 seconds for the model with a 12.7 mm (0.5 in.) mesh.

3. The single-degree-of-freedom models commonly used in practice are easy to use and require very short analysis times. However, they neglect modeling many important material behaviors and, thus, have much less reliability and accuracy. For the 10 analyses considered in this study, the SDOF models provided the least-accurate results with a mean of 1.17 and COV of 32% for the calculated-to-observed peak displacement ratios. These 10 analyses included simply-supported, single structural components, for which the SDOF methods were developed. When modeling more complex elements, which are common in practice, much less accurate results will be obtained.

4. The proposed analysis method accurately simulated the experimental behaviors of the specimens examined. Peak deflections, stiffnesses, residual deflections, and damage and failure modes were captured accurately. Considering all 24 simulations, a mean value of 1.02 and COV of 16% were obtained for the calculated-to-observed peak displacement ratios.

5. The proposed method requires simple structural models with line elements, uses default material models and analysis options, and requires short analysis times. For the specimens considered in this study, approximately 200 seconds was required per analysis.

6. Multiple successive analyses were successfully undertaken for the previously loaded specimens, taking the previous damage into account. For the second and third blast analyses, a mean value of 1.05 and COV of 13% were obtained.

7. The analysis results did not change considerably for the time-step lengths less than approximately the smallest vibration period, indicating this time-step length to be adequate.

8. A small amount of additional viscous damping, in the range of 1 to 2%, was required for the specimens subjected to very low blast pressures and thus exhibiting predominantly linear-elastic behaviors.

9. The default material models and numerical integration method of Wilson's Theta exhibited excellent convergence and numerical stability.

10. Analytical verification studies should be undertaken for shear-critical specimens to investigate the influence of shear effects on the computed response. The literature is currently lacking in experimental studies involving shear-critical elements subjected to blast loads.

11. A multi-linear blast pressure input should be developed to more accurately model the loading. Future work will include this development.

AUTHOR BIOS

ACI member Serhan Guner is an Assistant Professor in the Department of Civil Engineering at the University of Toledo, Toledo, OH. He received his PhD from the University of Toronto, Toronto, ON, Canada. He is a member of Joint ACI-ASCE Committee 447, Finite Element Analysis of Reinforced Concrete Structures. His research interests include finite element modeling of reinforced concrete structures, shear effects in concrete, development of analysis software, and structural response to impact, blast, and seismic loads.

ACKNOWLEDGMENTS

The author would like to thank G. Thiagarajan for providing the experimental photograph of one of the specimens examined in this study. The author would also like to acknowledge the contribution of H. Francisco Viana, an undergraduate summer student funded by the Science without Borders scholarship program, for assisting in the drafting and preparation of some of the figures used in this paper.

REFERENCES

- ABAQUS, 2015, "Analysis User's Manual," Dassault Systèmes, Providence, RI. <http://www.3ds.com/products-services/simulia/products/abaqus/> (last accessed July 18, 2015).
- Chak, I. N., 2013, "Janus: A Post-Processor for VecTor Analysis Software," MASC thesis, Department of Civil Engineering, University of Toronto, Toronto, ON, Canada, 193 pp.
- Dunkman, D. A.; Yousef, A. E. A.; Karve, P. M.; and Williamson, E. B., 2009, "Blast Performance of Prestressed Concrete Panels," *Proceedings of the 2009 Structures Congress: Don't Mess with Structural Engineers: Expanding Our Role*, pp. 1297-1306.
- fib Model Code, 2010, "fib Model Code for Concrete Structures," Ernst & Sohn, Oct. 2013, 434 pp.
- Guner, S., and Vecchio, F. J., 2008, "User's Manual of VecTor5," online publication, 88 pp. <http://www.ryerson.ca/sguner/Publications/UserManuals.html> (last accessed July 18, 2015).
- Guner, S., and Vecchio, F. J., 2010a, "Pushover Analysis of Shear-Critical Frames: Formulation," *ACI Structural Journal*, V. 107, No. 1, Jan.-Feb., pp. 63-71.
- Guner, S., and Vecchio, F. J., 2010b, "Pushover Analysis of Shear-Critical Frames: Verification and Application," *ACI Structural Journal*, V. 107, No. 1, Jan.-Feb., pp. 72-81.
- Guner, S., and Vecchio, F. J., 2011, "Analysis of Shear-Critical Reinforced Concrete Plane Frame Elements under Cyclic Loading," *Journal of Structural Engineering*, ASCE, V. 137, No. 8, pp. 834-843. doi: 10.1061/(ASCE)ST.1943-541X.0000346
- Guner, S., and Vecchio, F. J., 2012, "Simplified Method for Nonlinear Dynamic Analysis of Shear-Critical Frames," *ACI Structural Journal*, V. 109, No. 5, Sept.-Oct., pp. 727-737.
- Jacques, E., 2011, "Blast Retrofit of Reinforced Concrete Walls and Slabs," MASC thesis, Department of Civil Engineering, University of Ottawa, Ottawa, ON, Canada, 196 pp.
- LS-DYNA, 2015, "Keyword User's Manual," Livermore Software Technology Corporation, Livermore, CA. <http://www.lstc.com/products/ls-dyna> <http://www.lstc.com/download/manuals/> (last accessed July 18, 2015).

Malvar, L. J., 1998, "Review of Static and Dynamic Properties of Steel Reinforcing Bars," *ACI Materials Journal*, V. 95, No. 5, Sept.-Oct., pp. 609-614.

Newmark, N. M., 1959, "A Method of Computation for Structural Dynamics," *Journal of the Engineering Mechanics Division*, ASCE, V. 85, No. 3, May-June, pp. 67-94.

PDC, 2015, "SBEDS: Single-Degree-of-Freedom Blast Effects Design Spreadsheet," Protective Design Centre, U.S. Army Corps of Engineers, Vicksburg, MS, <https://pdc.usace.army.mil/software/sbeds/> (last accessed July 18, 2015).

Robert, S. D., and Johnson, C. F., 2009, "Blast Response of Conventional and High Performance Reinforced Concrete Panels," *Proceedings of the 2009 Structures Congress: Don't Mess with Structural Engineers: Expanding Our Role*, Austin, TX, pp. 1142-1150.

Sadeghian, V., 2012, "Formworks-Plus: Improved Pre-Processor for Vector Analysis Software," MSc thesis, Department of Civil Engineering, University of Toronto, Toronto, ON, Canada, 147 pp.

Shetye, G. A., 2013, "Finite Element Analysis and Experimental Validation of Reinforced Concrete Single-Mat Slabs Subjected to Blast Loads," MSc thesis, Department of Civil Engineering, University of Missouri-Kansas City, Kansas City, MO, 155 pp.

Thiagarajan, G., and Johnson, C. F., 2014, "Experimental Behavior of Reinforced Concrete Slabs Subjected to Shock Loading," *ACI Structural Journal*, V. 111, No. 6, Nov.-Dec., pp. 1407-1417. doi: 10.14359/51686970

Thiagarajan, G.; Kadambi, A. V.; Robert, S.; and Johnson, C. F., 2015, "Experimental and Finite Element Analysis of Doubly Reinforced Concrete Slabs Subjected to Blast Loads," *International Journal of Impact Engineering*, V. 75, pp. 162-173. doi: 10.1016/j.ijimpeng.2014.07.018

Thiagarajan, G.; Vasudevan, A. K.; and Robert, S., 2011, "Numerical Modeling of Concrete Slabs Reinforced with High Strength Low Alloy Vanadium Steel Bars Subjected to Blast Loads," *Behavior of Concrete Structures Subjected to Blast and Impact*, SP-281, American Concrete Institute, Farmington Hills, MI, pp. 263-277.

Vasudevan, A. K., 2012, "Finite Element Analysis and Experimental Comparison of Doubly Reinforced Concrete Slabs Subjected to Blast Loads," MSc thesis, Department of Civil Engineering, University of Missouri-Kansas City, Kansas City, MO, 74 pp.

Vecchio, F. J., 2000, "Disturbed Stress Field Model for Reinforced Concrete: Formulation," *Journal of Structural Engineering*, ASCE, V. 126, No. 9, pp. 1070-1077. doi: 10.1061/(ASCE)0733-9445(2000)126:9(1070)

Wilson, E. L.; Farhoomand, I.; and Bathe, K. J., 1972, "Nonlinear Dynamic Analysis of Complex Structures," *Journal of Earthquake Engineering & Structural Dynamics*, V. 1, No. 3, pp. 241-252. doi: 10.1002/eqe.4290010305

Wong, P. S.; Vecchio, F. J.; and Trommels, H., 2013, "VecTor2 and FormWorks User's Manual," *Technical Report*, Department of Civil Engineering, University of Toronto, Toronto, ON, Canada, 318 pp.